Hindawi
Journal of Nanomaterials
Volume 2022, Article ID 7529036, 10 pages
https://doi.org/10.1155/2022/7529036

Research Article

Biogas Production from Food Waste Using Nanocatalyst

P. Bharathi,[1] **R. Dayana**,[2] **Magesh Rangaraju**,[3] **V. Varsha**,[4] **M. Subathra**,[4] **Gayathri**,[4] **and Venkatesa Prabhu Sundramurthy**[5,6]

[1]*Bharath Institute of Higher Education and Research, Selaiyur, Chennai, India*
[2]*SRM Institute of Science and Technology, Kattankulathur, Chennai, India*
[3]*Department of Chemical Engineering, Wachemo University, Hossana, Ethiopia*
[4]*Karpaga Vinayaga College of Engineering and Technology, Chinnakolambakkam, India*
[5]*Department of Chemical Engineering, College of Biological and Chemical Engineering, Addis Ababa Science and Technology University, Ethiopia*
[6]*Center of Excellence for Bioprocess and Biotechnology, Addis Ababa Science and Technology University, Ethiopia*

Correspondence should be addressed to P. Bharathi; bharathipurush@gmail.com, R. Dayana; dayanar@srmist.edu.in, and Venkatesa Prabhu Sundramurthy; venkatesa.prabhu@aastu.edu.et

Received 18 May 2022; Revised 18 June 2022; Accepted 24 June 2022; Published 31 July 2022

Academic Editor: Lakshmipathy R

The food waste management has become a very important part in the modern world. In the olden days, the population was very low, so that the low waste produced was easily disposed by dumping it under the soil. However, nowadays, due to high population, amount of waste is produced high which could not be dumped due to the land pollution. To overcome this problem, the food waste must be managed or utilized properly to give zero waste. Therefore, this work focused on the production of biogas from food waste through the anaerobic digestion process using iron oxide nanoparticles. The iron oxide nanocatalyst from red mud reduced the process time for the anaerobic digestion was by 5.38% compared to the noncatalytic process. The produced biogas analysis done through GCMS analysis and calculated by comparing the both anaerobic degradation setup with and without nanocatalyst. Nanocatalyzed degradation contains 50% high amount of methane and 23.5% of total amount of biogas when compared to nonnanocatalyzed degradation.

1. Introduction

Food waste management is the biggest challenge in the modernized world, because in olden days the wastes were dumped under the landfills due to lesser population and higher availability of land area. The food wastes largely produced through markets, agricultural fields, transportation, hotels, food factories, and marriage halls. The produced food wastes are disposed through land filling and dumped in the open environment by an improper way. The dumped food wastes slowly start degrading with fouling odor and emit greenhouse gases like methane and carbon dioxide. Global warming potential of methane gas was twenty-one times higher than the carbon dioxide [1]. The emission of the greenhouse gases leads to severe global warming and create adverse effects to the environment. The fouling odor comes from the dumped food wastes create sanitation problems. To overcome the above problems, the present research work focused on to produce biogas from food waste using a nanocatalyst. Generally, the iron oxide nanoparticles serve in the electron exchange process which consequently enhances the whole anaerobic digestion process [2]. It possess a peculiar property of stimulating the bacterial growth which helps to reduce the retention time for digestion process and simultaneously increases the biogas production. For the mentioned above reasons only, the iron oxide nanoparticles were chosen for this study. In this project, the main aim is to obtain value added products from waste.

Biogas can also produce from the water hyacinth, which would provide the innovative way for the renewable energy. This also prevents the invasion of weed in the fresh water bodies [3]. Biogas was also produced from macro algae by

anaerobic digestion process which produced methane in a percentage around 46.5% to 36.9% [4]. To produce biogas, the anaerobic digestion process is widely carried out because of its huge advantages which include low sludge production, low energy consumption, small area requirement, reduction of volume of solid waste, and production of biofertilizer [5].

Even though lot of biogas plant has been constructed in rural areas to manage the waste, many of them survive as a failure model due to many parameters such as retention time, consistency in gas production, and less yield [6]. The major problem of household biogas plant over in size and cannot overcome the sudden reduction in feed stock amount [7]. To reduce these difficulties, nanoparticles emerged into this field. Ni and Co nanoparticles used to increase the digestion rate of waste leading to higher biogas production [8]. From the previous studies, methane production enhanced by treating the sludge with iron oxide nanoparticle and multiwalled carbon nanotubes [9]. Calcium peroxide catalyst the anaerobic digestion of food waste, cow dung, and sludge solution to produce hydrogen and methane [10]. The role of catalyst in increase of biogas production through anaerobic co digestion process. It was reported that iron plays a role as catalyst and increases the production of biogas from organic wastes through anaerobic codigestion process [11].

In general, metal nanoparticles require higher time for degradation process. These metals are sometimes hazardous to the environment [6]. By considering that, in the present work, the iron (raw material for nanoparticle synthesis) separated and isolated from the red mud and after the biogas production from nanocatalyzed degradation the leftover slurry processed as a biofertilizer.

The main objective of the present research was to synthesize and characterize the iron oxide nanoparticles, and it was used as a catalyst at anaerobic degradation of food waste to produce biogas.

2. Materials and Methodology

2.1. Synthesis of Iron Oxide Nanoparticles. The red soil was taken as the source of iron. This work reported that iron normally present high amount in soil but they are very poorly soluble in nature and it associated with other minerals [12].

The soil roasted at 300°C for 1 hour for easy separation of iron by mechanical method. The process parameters fixed by optimizing the time, temperature, and concentration of the iron for the reduction of iron-to-iron oxide nanoparticles. Three grams of separated iron weighed and mixed with 1 : 2 : 2 : 8 ratios of concentrated diluted hydro chloric acid, ethyl acetate, glycerol, and distilled water [6]. The mixture stirred at 60°C for 24 hours to reduce the bulk iron into iron oxide nanoparticles. The nanoparticles removed by centrifugation and washed with ethanol thrice. The purified nanoparticles dried at 100°C and stored for further use.

2.2. Characterization of Iron Oxide Nanoparticles. The synthesized nanoparticles were characterized by UV-Vis spectrophotometry to find the maximum absorbance value. The molecules present in the solution has a capacity in absorbing the UV or visible light. By measuring the absorbance, the concentration of the solution can be determined. Fourier transform infrared spectroscopy (FTIR) was used to find the functional group of the synthesized nanoparticles. As like UV-Visible spectrophotometry, FTIR uses infrared rays to generate the peak values. By comparing, the peak values with the FTIR database, the functional group of the organic and inorganic substances can be determined. Crystalline phases and morphology can be studied by scanning electron microscopy and obtained particle size at 100 nm [13]. The size and shape of the molecule can be determined efficiently from this analysis. Energy dispersive X-ray analysis (EDAX) carried out to find the elemental composition of the synthesized iron oxide nanoparticles by using X-ray, which passes through the sample and exit the electron found on the surface of the molecule. This X-ray passes through the detector to generate the data on the screen. The iron oxide nanoparticles were synthesized by simple precipitation method and studied the optical properties by UV-visible and FT-IR spectra. The nanoparticles were characterized by X-ray diffraction method, and Scherer formula was used to calculate the grain size of the nanoparticle [14].

2.3. Collection and Processing of Food Waste. Two different wastes are food waste and market waste which have been collected from BIHER college mess, canteen, pantry areas, vegetables, and fruit market in and around the areas of Chennai. These wastes were grinded well and underwent for degradation process.

2.4. Optimization of Waste for Higher Biogas Yield. Optimization carried out among six different combinations of the waste. The first bottle was filled with 5 : 1 ratio of food waste and cow dung. The second bottle was filled with 5 : 1 ratio of market waste and cow dung. The third bottle was filled with 2.5 : 2.5 : 1 ratio of food waste, market waste, and cow dung. The fourth and fifth bottles were filled with food waste and market waste. The sixth bottle was filled with 1 : 1 ratio of food waste and market waste. In all the bottles, water was added two times the volume of the slurry and mixed well. The bottles were connected to the water displacement setup so that the produced biogas can easily measure. The setup was placed under dark for anaerobic degradation process. The quantitative and qualitative parameters of biogas were analyzed for all the setup.

2.5. Optimization of pH and Iron Oxide Nanoparticles in the Biogas Production. pH and the iron oxide nanoparticles play a major role in the degradation process, which stimulates biogas production and the retention time of the degradation process. The optimized source was taken in the same ratio and mixed with water in double the volume of the slurry. By following the same ratio, 10 nos. of 300 ml bottles were filled. Among the 10 bottles, 5 bottles were taken for pH optimization. pH was altered by adding acetic acid ranging from 4 to 1 ml in 4 bottles. Fifth bottle was maintained with the original pH (4.5, 5.1, 5.7, 6.3, and 7 pH of all 5 bottles). Next, a set of 5 bottles were taken for nanoparticle optimization. Nanoparticles added in concentration of 10 mg/100 ml

Table 1: Optimization of waste for higher biogas production.

Bottle no	Source	3rd day	6th day	9th day	12th day	15th day	18th day	21st day
1	FW+CD	120 ml	135 ml	90 ml	90 ml	45 ml	10 ml	Trace amount
2	MW+CD	159 ml	144 ml	135 ml	150 ml	51 ml	17 ml	Trace amount
3	FW+MW+CD	195 ml	180 ml	210 ml	195 ml	60 ml	20 ml	10 ml
4	FW	60 ml	75 ml	66 ml	72 ml	29 ml	8 ml	Trace amount
5	MW	75 ml	105 ml	96 ml	98 ml	39 ml	13 ml	Trace amount
6	FW+MW	96 ml	120 ml	115 ml	105 ml	43 ml	13 ml	Trace amount

FW: food waste; MW: market waste; CD: cow dung.

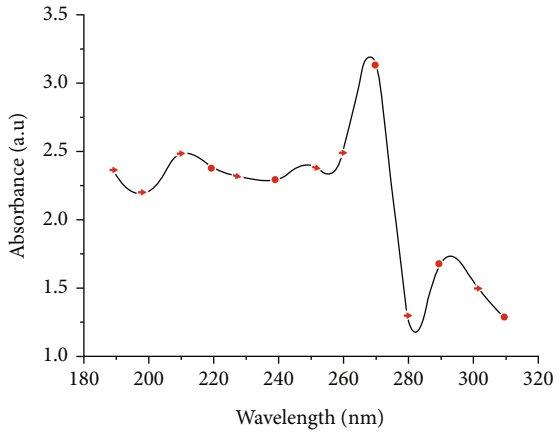

Figure 1: UV analysis of iron oxide nanoparticles (maximum absorbance at 272 ± 5 nm).

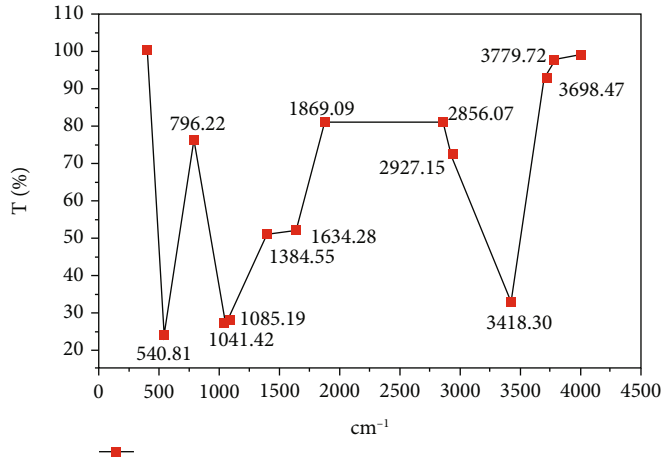

Figure 2: FTIR peak values of iron oxide nanoparticles.

to 40 mg/100 ml. The last bottle was fixed as control without any addition of nanoparticles. All the bottles were setup by water displacement method and kept under dark for anaerobic digestion. After 2 days, the produced gas quantity was noticed. By comparing the quantity of biogas produced in each batch, the optimum pH and concentration of nanoparticles were fixed by based on the highest biogas produced.

2.6. Pilot Scale Setup. The optimized source, pH, and concentration of nanoparticle was encountered in the pilot scale setup for the biogas production. Here, two setups were made, one with nanocatalyzed degradation and another noncatalyzed degradation process. Both the setups were kept under dark for 5 days to complete degradation of slurry. The produced biogas were analyzed to make a comparative study over the nanoparticle catalyzed and noncatalyzed reactions.

2.7. Gas Analyzer. Mass spectrometry was carried out to find the structural formula of the compounds present in the gas along with their respective percentage calculated from their peak value and its corresponding area value. Another method is to measure the CO_2 content in the produced biogas by using NaOH solution. Hence, 5 ml of gas was taken via syringe into that 10 ml of NaOH was sucked and shaken

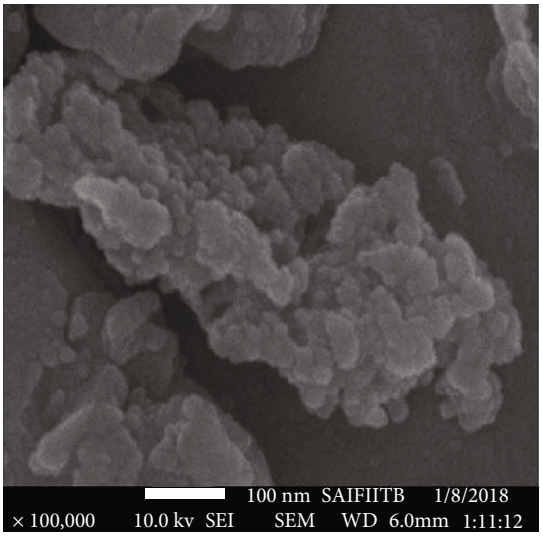

Figure 3: SEM image of iron oxide nanoparticles.

Element	weight%	Atomic%
O K	30.88	60.94
Fe K	69.12	39.06
Totals	100.00	

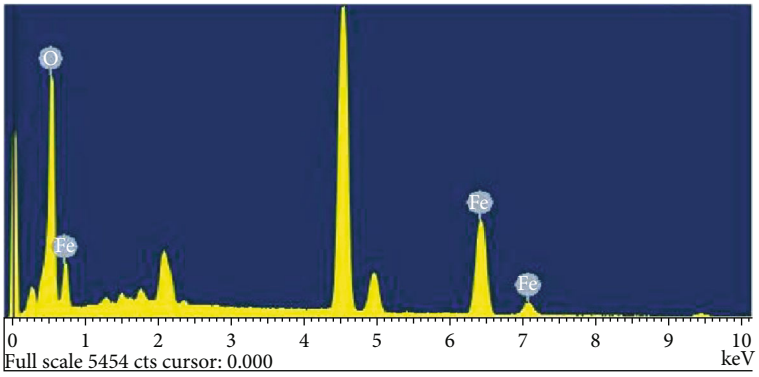

Figure 4: EDAX of synthesized iron oxide nanoparticles.

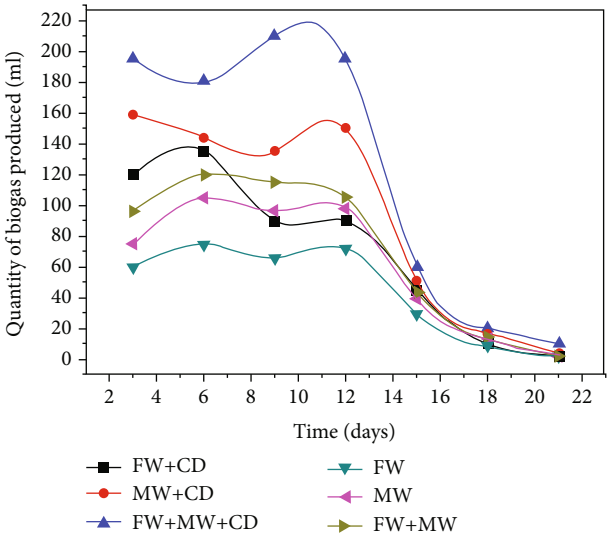

Figure 5: Optimization of waste for higher biogas production. FW: food waste; MW: market waste; CD: cow dung.

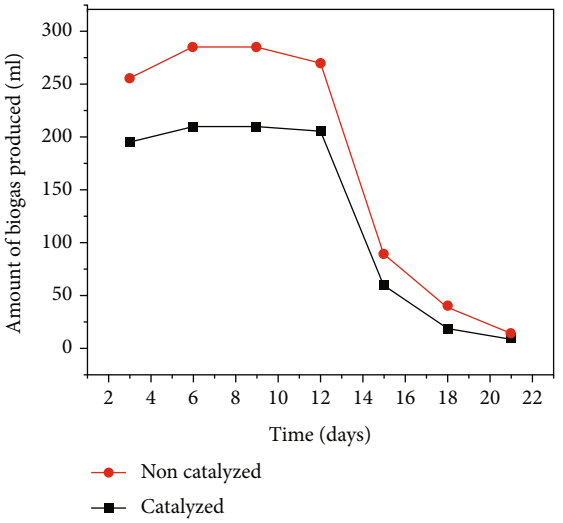

Figure 6: Biogas production for the catalyzed and noncatalyzed processes.

Table 2: Biogas yield in both the catalyzed and noncatalyzed processes.

Bottle no	Source	3rd day	6th day	9th day	12th day	15th day	18th day	21st day
1	FW+MW+CD	195 ml	210 ml	210 ml	206 ml	60 ml	20 ml	10 ml
2	FW+MW+CD	255 ml	285 ml	285 ml	270 ml	90 ml	40 ml	15 ml

FW: food waste; MW: market waste; CD: cow dung.

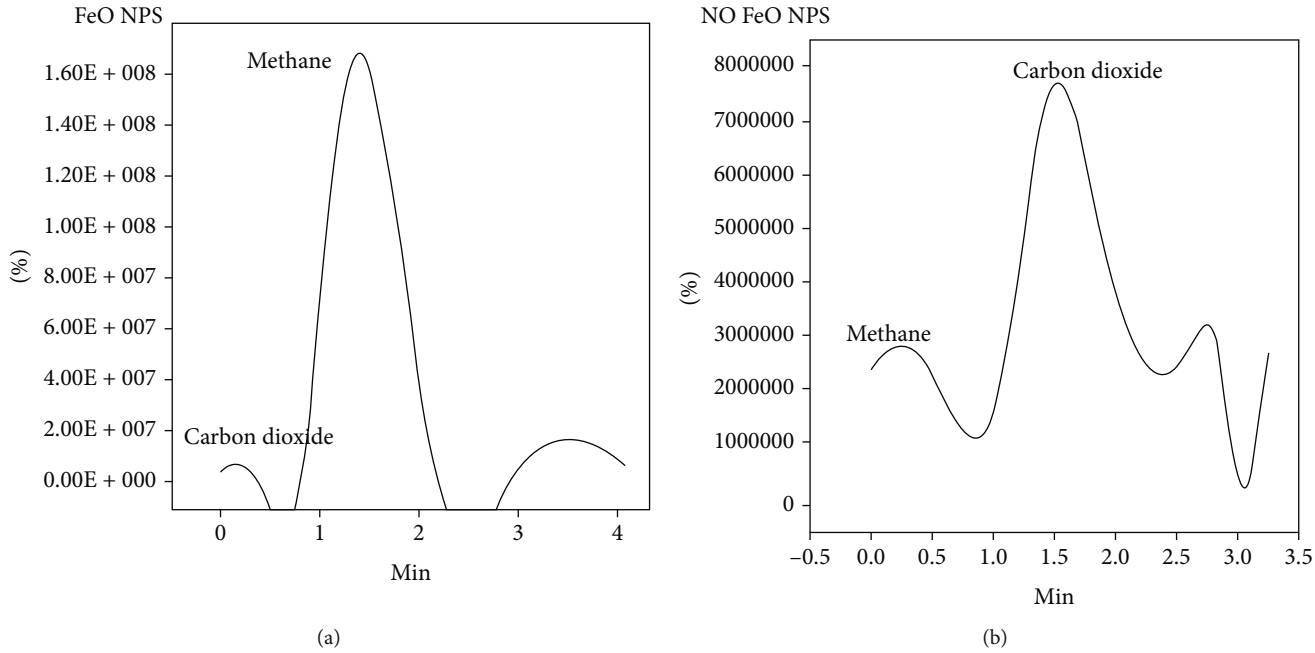

Figure 7: Gas chromatography graph of biogas (a) with and (b) without iron oxide nanoparticles.

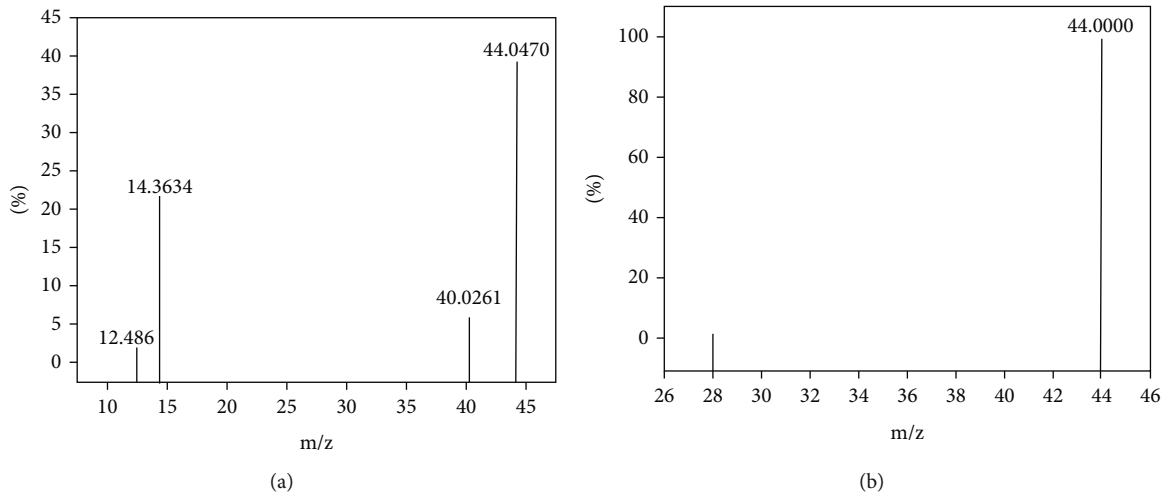

Figure 8: Components of biogas in GCMS analysis.

well. 10 ml of the liquid from the syringe was discarded, and leftover gas and water were measured. The remaining water present in the syringe indicates the presence of CO_2 present in the biogas produced because CO_2 react with the NaOH to give away water. The remaining gas represents the percentage of methane and trace amount of the nitrogen and hydrogen present in the biogas.

3. Result and Discussion

The iron oxide nanoparticles were synthesized by polyol method, which appeared black in color and possessed magnetic property, which was confirmed by attracting the synthesized nanoparticles present in the solution by the magnet. Normally, iron oxide nanoparticle synthesis was

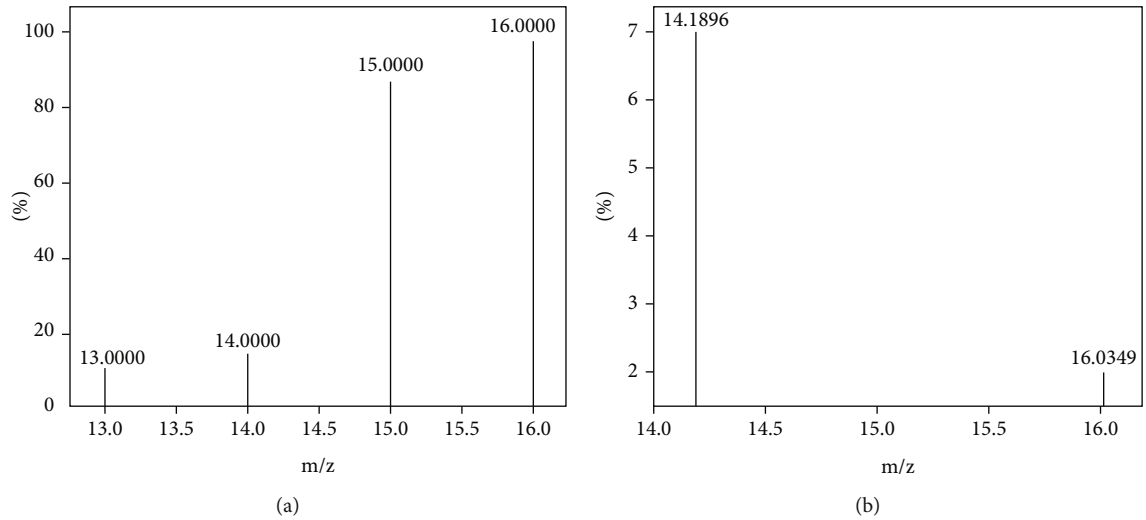

Figure 9: Mass spectrometry graph of carbon dioxide composition in biogas with (a) and without (b) a nanocatalyst.

Table 3: Composition of biogas: (a) GCMS analysis and (b) NaOH analysis.

(a) GCMS

S.no	Gas composition	Anaerobic degradation with catalyst	Anaerobic degradation without catalyst
1	CH_4	59.85%	32%
2	CO_2	40.14%	68%
3	H_2O	2.6%	5.26%
4	H_2S	1.4%	1.82%

(b) NaOH

S.no	Gas composition	Anaerobic degradation with catalyst	Anaerobic degradation without catalyst
1	CH_4	60%	30%
2	CO_2	40%	70%

done by 2-3 days. Chemical synthesis of iron oxide nanoparticle was carried out by using ferric chloride as a precursor in which the yellow color changes to dark brown color which indicates the reduction reaction takes place [6]. Size-specific iron nanoparticles produced by pulsed laser ablation were also available [15]. Coating of sand over the iron oxide nanoparticles by biological method was also experimented [16].

3.1. Characterization of Iron Oxide Nanoparticles. The maximum absorbance of iron oxide nanoparticles was found to be 270 ± 5 nm by UV-Vis spectrophotometry analysis [14]. The optimized values have been presented in Table 1. A synthesized iron oxide nanoparticle from ferric chloride by chemical method in which maximum absorbance noted as 272 nm was shown in Figure 1. FTIR analysis was done for the synthesized nanoparticles. The obtained peak values are representing the corresponding functional groups by comparing the peak values with the standard database. The obtained peak values are 3779, 3698, 2927, 2856, 1869, 1041, 796, and 779 represents the aromatic and aliphatic amines and 3418, 1384, and 540 peaks are corresponding to hydroxyl-stretching group shown in Figure 2 [14]. The peaks of 3789, 3005, and 1092 indicating iron oxide nanoparticles, which coincide with the peak value of synthesized nanoparticles that represent the aromatic or aliphatic amines. The peak value of 552 and 1361 represents the hydroxyl group; it coincided with the results.

The SEM image (Figure 3) was clearly representing the structural property of the synthesized nanoparticles. The appearance is clearly proved by the crystalline nature of the iron oxide nanoparticles.

The particles are found to be aggregated with one another, and it was clearly shown that the size ranges from 10 to 90 nm. Some authors focused on the sand-coated iron oxide nanoparticles, which appeared spherical in shape [16]. The colloidal iron nanoparticles were prepared by using acetone and water. Here, the growth time was reduced due to the presence of liquid confinement whose size was 30 nm for acetone solvent and 27 nm for water as discussed [15]. Sonochemically synthesized gamma iron oxide nanoparticles were visualized by SEM where it was aggregated with one another as confirmed [17].

EDAX (energy dispersive X-ray analysis) was carried to find out the elemental composition of the synthesized

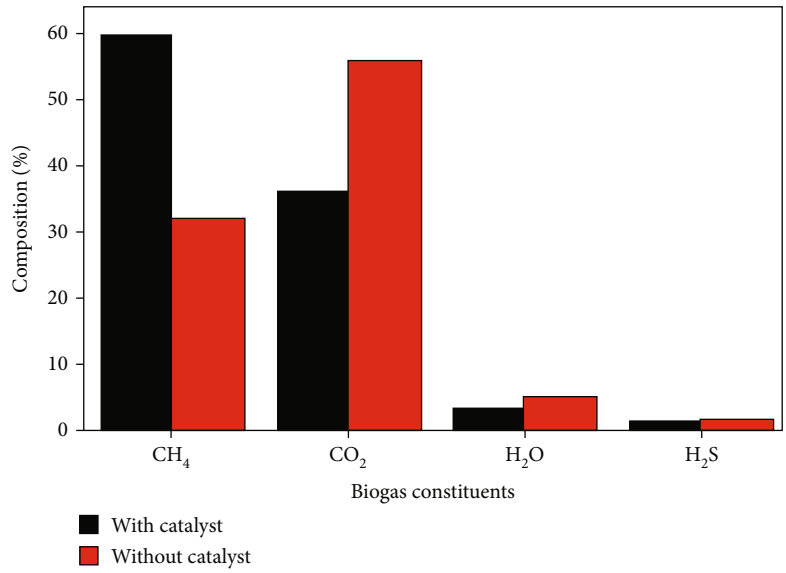

Figure 10: Mass spectrometry graph of methane in biogas with (a) and without (b) a nanocatalyst.

nanoparticles. The spectrum result confirms the strong peaks of iron and oxide, in which 69.12% of iron and 30.88% of oxide found in the sample. From the percentage of the iron and oxide present in the synthesized nanoparticles, the molecular formula was determined as Fe_2O shown in Figure 4. One of the previous report of EDS analysis showed that the value for the iron oxide nanoparticles was 73.36% of iron and 21.02% of oxide obtained [18].

3.2. Optimization of Waste for Higher Biogas Production. As shown in Figure 5, six different setups were made to undergo the degradation process, and thus, biogas was produced. The biogas production was measured daily by water displacement method. The food waste, market waste, and cow dung combination produced higher biogas with lesser time compared than other combination of source. The third bottle source was fixed for bulk production. Different wastes were used as a raw material for the biogas production such as algae with aquatic plants, industrial waste, municipal solid waste, food waste, cellulosic waste, agricultural waste, livestock waste, and sewage sludge. Among the above, sewage sludge has a predominant source [19]. Mixture of different raw materials was also used for the biogas production such as cow dung, pig manure, cow urine, and fecal matter [7]. Maize and silage were also used as the raw materials for the biogas production among which silage have higher biogas yield compared to maize [20].

3.3. Optimization of pH and Iron Oxide Nanoparticle in Biogas Production. The optimization of pH and concentration of the nanoparticle was finalized by the high amount of gas production on the water displacement method. Based on that, high yield of biogas was calculated at original pH of the sample compared to the reduced pH. The reason of pH value was not increased more than 7 is because the biofertilizer pH value must lie between 4.5 and 7.5 for major number of plants since the slurry left over after the biogas production will be used as a biofertilizer, and it was reported as different pH ranging from 7.4 to 8.5 [3].

Table 4: Compounds in mass spectrometry.

S.no	Atomic mass number	Compounds
1	16	Methane
2	44	Carbon dioxide
3	14	Nitrogen
4	12	Carbon

The nanoparticle concentration also fixed in the same way by observing the amount of biogas produced in the water displacement method and 3% of used in this study. Above the 3% of iron oxide nanoparticles not much increase in rate of anaerobic digestion process. Minimum of 40 ppm and maximum of 100 ppm of iron oxide nanoparticle were used as a catalyst for the degradation process [6].

3.4. Pilot Scale Setup. FW+MW+CD combinations were undergoing pilot scale setup for both nanocatalyzed and nonnanocatalyzed degradation processes. The biogas produced at the time of degradation process starts being measured by water displacement method. The feed 700 grams produced 891 ml of biogas via noncatalyzed degradation process while the catalyzed degradation process produced 1165 ml of biogas after 21 days. Initial biogas production observed after 12 hours in the noncatalytic process whereas the biogas production observed within 8 hours via catalytic degradation process. The biogas was giving more yield at the early days of degradation when compared to the end. The rate of degradation simultaneously increases the biogas production. As shown in Figure 6, the amount of biogas production measured with respect to the days in that the nanocatalyzed digestion showed more biogas production than the nonnanocatalyzed digestion. The biogas production was

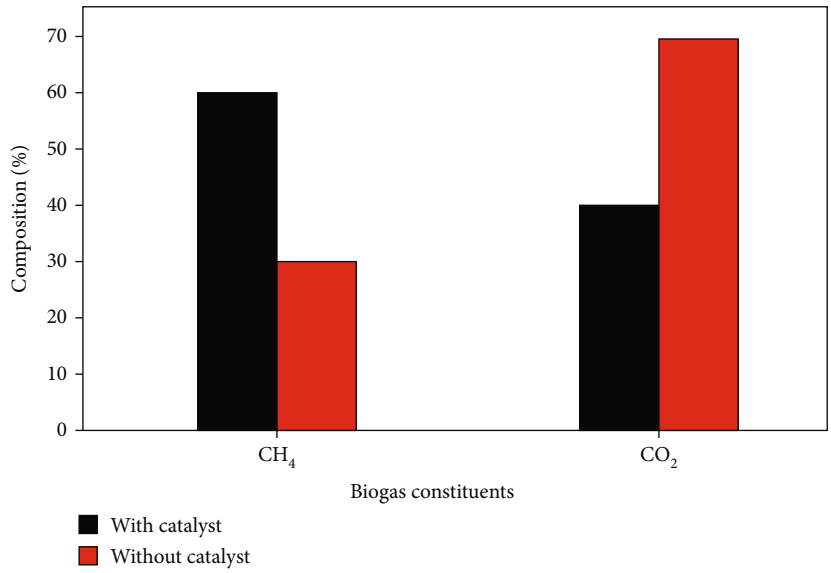

Figure 11: Components of biogas in NaOH analysis.

gradually decreasing with a greater number of days. The corresponding values of the graph were shown in Table 2. Silage and maize were used as the feed for biogas production [20] and here used 450 grams of feed to give 605 ml of biogas at the end of 12^{th} day. Biogas production noted for different algal species like *Cladophora glomerata*, *Chara fragilis*, and *Spirogyra neglecta* for 15 days in which *Spirogyra neglecta* gave maximum yield [4].

3.5. Gas Analysis. The biogas produced through the anaerobic degradation process with and without catalyst was analyzed by GC-MS (Figure 7). Through analysis, the data compounds were present in biogas was found to be methane, carbon dioxide, nitrogen, and trace amounts of hydrogen sulfide presents in both the nanocatalyzed and noncatalyzed degradation processes. The percentage of the compounds were present in the produced biogas calculated from the peak area value and the comparison shown in Figure 8. Among the peaks generated, only carbon dioxide and methane peaks were considered since it is the most important compounds for the biogas. In the noncatalyzed degradation process, the production of carbon dioxide was noted high compared to the methane. 68% of carbon dioxide and 32% of methane were calculated from the peak area values, whereas the catalyzed degradation process 40.14% of carbon dioxide and 59.85% of methane calculated from the graphical peak area values. As shown in Figure 9, the gas chromatography graph of the produced biogas with and without nanocatalyst from peaks the composition of individual compounds was calculated by measuring the (height of the peak × width of the peak at half height by total area) and it was tabulated in Table 3(a). The time taken for the production of biogas via catalyzed process was reduced to 5.38% compared with noncatalyzed process. Therefore, the amount of methane was produced and found to be higher than the carbon dioxide production, which indicates the efficiency of biogas is higher in catalyzed reaction than the noncatalyzed reaction. The mass spectrometry graph of the produced biogas was shown on Figures 9 and 10. In Figure 9, the composition of carbon dioxide and the related compounds were confirmed. In Figure 10, the composition of methane on both the catalyzed and noncatalyzed processes were confirmed, and it was tabulated in Table 4.

3.6. The NaOH Test. The NaOH test was carried out to find out the amount of carbon dioxide present in the produced biogas (Figure 11). In this test, the noncatalyzed biogas was given 3.5 ml of water and 2 ml of gas. It confirms that 70% of CO_2 and 30% of the methane was present in the biogas produced. In nanocatalyzed reaction, 2 ml of water and 3 ml of gas remains after the reaction, which indicates the presence of 40% of CO_2 and 60% of methane, nitrogen, and hydrogen gas was tabulated on Table 3(b). The NaOH test was compared with the GCMS percentage calculation, which was more or less similar. The biogas production was carried out from the food waste with catalyst were 5% of carbon dioxide production was found less in the catalyst process compared to the noncatalyzed process [6].

4. Conclusions

The synthesized nanoparticle was iron confirmed by UV spectroscopy. The obtained nanoparticle size was 100 nm, characterized through SEM and TEM analyses. Synthesized nanoparticles contained 69.12% iron and 30.88% oxide by EDAX analysis. Nanoparticles are used as a catalyst on anaerobic degradation of food waste to produce biogas. Metallic catalysts (Ni, Fe, Cu, etc.) are involved in enhancing the methane conversion at a lower temperature. However, these metallic catalysts lose their activity very fast [21]. 891 ml of biogas from noncatalytic induced degradation process while the catalytic degradation process produced 1165 ml of biogas on 21 days. The biogas produced from

the nanocatalyzed anaerobic degradation of waste (food waste+market waste+cow dung) gives 46.5% higher amount of methane compared to the noncatalyzed process from GCMS analysis. Total amount of biogas production on 21 days was 23.5% high at nanocatalyzed anaerobic process compared to nonnanocatalyzed fertilizer. The nanocatalyst also reduces the process time of anaerobic degradation by 5.38%. Novelty of this work is one of the oligoelements of iron oxide nanoparticles are able to rise the efficiency of methanogenesis. Mostly, it acts as coenzymes in biochemical processes and enhances the methanolic activity of methanogens. From, the above results, the nanocatalyst (iron oxide nanoparticles) makes the degradation process faster and simultaneously increases the biogas production.

Abbreviations

CO_2:	Carbon dioxide
Ni:	Nickel
Co:	Cobalt
FTIR:	Fourier transform infrared spectroscopy
UV:	Ultraviolet
HCl:	Hydrochloric acid
SEM/EDAX:	Scanning electron microscopy and energy dispersive spectroscopy
EDS:	Energy dispersive X-ray spectroscopy
NaOH:	Sodium hydroxide
Ppm:	Parts per million.

Data Availability

The underlying data supporting the results of the study presented in this paper.

Conflicts of Interest

The authors declare that they have no conflicts of interest.

References

[1] A. Sulaiman, N. Othman, A. S. Baharuddin, M. N. Mokhtar, and M. Tabatabaei, "Enhancing the halal food industry by utilizing food wastes to produce value-added bioproducts," *International Halal Conferences*, vol. 121, pp. 35–43, 2014.

[2] Y. Liu, Y. Zhang, and B. J. Ni, "Zero valent iron simultaneously enhances methane production and sulfate reduction in anaerobic granular sludge reactors," *Water Research*, vol. 75, pp. 292–300, 2015.

[3] P. Njogu, R. Kinyua, P. Muthon, and Y. Nemoto, "Biogas production using water hyacinth (Eicchornia crassipes) for electricity generation in Kenya," *Energy and power Engineering*, vol. 7, no. 5, pp. 209–216, 2015.

[4] P. Baltrenas and A. Misevicius, "Biogas production experimental research using algae," *Baltrėnas and Misevicius Journal of Environmental Health Science and Engineering*, vol. 13, no. 1, pp. 13–18, 2015.

[5] K. F. Adekunle and J. A. Okolie, "A review of biochemical process of anaerobic digestion," *Advances in Bioscience and Biotechnology*, vol. 6, no. 3, pp. 205–212, 2015.

[6] K. M. Sreekanth and D. Sahu, "Effect of iron oxide nanoparticle in bio digestion of a portable food-waste digester," *Journal of Chemical and Pharmaceutical Research*, vol. 7, no. 9, pp. 353–359, 2015.

[7] P. Tumutegyereize, C. Ketlogetswe, J. Gandure, and N. Banadda, "Technical evaluation of uptake, use, management and future implications of household biogas digesters—a case of Kampala city peri-urban areas," *Computational Water, Energy, and Environmental Engineering*, vol. 6, no. 2, pp. 180–191, 2017.

[8] E. Abdelsalam, M. Samer, Y. A. Attia, M. A. Abdel-Hadi, H. E. Hassan, and Y. Badr, "Comparison of nanoparticles effects on biogas and methane production from anaerobic digestion of cattle dung slurry," *Energy Conversion and Management*, vol. 87, pp. 592–598, 2016.

[9] J. J. Ambuchi, Z. Zhang, and Y. Feng, "Biogas enhancement using iron oxide nanoparticles and multi-wall carbon nanotubes," *International Journal of Chemical, Molecular, Nuclear, Materials and Metallurgical Engineering*, vol. 10, p. 10, 2016.

[10] C. Deheri and S. K. Acharya, "An experimental approach to produce hydrogen and methane from food waste using catalyst," *International Journal of Hydrogen Energy*, vol. 45, pp. 17250–17259, 2020.

[11] S. H. Joo, L. Delicio, J. Muniz, and S. Baek, "Perspective: catalytic increase of biogas production in an anaerobic co-digestion system," *International Journal of Nanoparticles and Nanotechnology*, vol. 4, no. 1, pp. 1–6, 2018.

[12] T. Mimmo, D. Buono, R. Terzano, N. Tomasi, G. Vigani, and R. Crecchio, "Rhizospheric organic compounds in the soil-microorganism-plant system their role in iron availability," *European Journal of Soil Science*, vol. 65, no. 5, pp. 629–642, 2014.

[13] J. C. de Freitas, R. M. Branco, I. G. O. L. T. P. da Costa, M. G. N. Campos, M. J. Junior, and R. F. C. Marques, "Magnetic nanoparticles obtained by homogeneous coprecipitation sonochemically assisted," *Materials Research*, vol. 18, Supplement 2, pp. 220–224, 2015.

[14] K. Tharani and L. C. Nehru, "Synthesis and characterization of iron oxide nanoparticles by precipitation method," *International Journal of Advanced Research in Physical Science (IJARPS)*, vol. 2, pp. 47–50, 2015.

[15] S. Dadashi, R. Poursalehi, and H. Delavari, "Structural and optical properties of pure iron and iron oxide nanoparticles prepared via pulsed Nd: YAG laser ablation in liquid," *Procedia Materials Science*, vol. 11, pp. 722–726, 2015.

[16] V. Raiza Rasheed Meera, "Synthesis of iron oxide nanoparticles coated sand by biological method and chemical method," *Procedia Technology*, vol. 24, pp. 210–216, 2016.

[17] S. F. Hasany, J. I. Ahmed Rajan, and A. Rehman, "Systematic review of the preparation techniques of iron oxide magnetic nanoparticles," *Nanoscience and Nanotechnology*, vol. 2, no. 6, pp. 148–158, 2012.

[18] P. L. Hariani, M. Faizal, R. Ridwan, M. Marsi, and D. Setiabudidaya, "Synthesis and properties of Fe_3O_4 nanoparticles by co-precipitation method to removal procion dye," *International Journal of Environmental Science and Development*, vol. 4, no. 3, pp. 336–340, 2013.

[19] R. L. Grando, F. V. da Fonseca, and A. M. de Souza Antunes, "Mapping of the use of waste as raw materials for biogas production," *Journal of Environmental Protection*, vol. 8, no. 2, pp. 120–130, 2017.

[20] P. Satpathy, S. Steinigeweg, E. Siefert, and H. Cypionka, "Effect of lactate and starter inoculum on biogas production from fresh maize and maize silage," *Advances in Microbiology*, vol. 7, no. 5, pp. 358–376, 2017.

[21] L. Goswami, A. Kushwaha, A. Singh et al., "Nano-Biochar as a sustainable catalyst for anaerobic digestion: a synergetic Closed-Loop approach," *Recent Advances on Nano Catalysts for Biological Processes*, vol. 12, pp. 186–193, 2022.